Japan Journal of Research

Review Article

The Switching Mechanisms of Dihydroazulene/Vinylheptafulvene Photo-/Thermoswitches

Anders S. Gertsen and Kurt V. Mikkelsen

Department of Chemistry, University of Copenhagen, Universitetsparken 5, 2100 Copenhagen Ø, Denmark

Correspondence

Kurt V Mikkelsen

Department of Chemistry, University of Copenhagen, Universitetsparken 5, 2100 Copenhagen Ø, Denmark

E-mail: kmi@chem.ku.dk

- Received Date: 25 Jul 2023
- Accepted Date: 31 Jul 2023
- Publication Date: 03 Aug 2023

Abstract

We have investigated the switching mechanisms of photochromic systems that are relevant for harvesting, storing, and releasing solar energy. We consider storage of solar energy in the form of energetic chemical bonds via light-induced isomerization reactions. The approach concerns photoswitches that upon irradiation isomerize to high-energy metastable isomers and through the corresponding back-reaction will release the stored energy. Thereby, we have considered molecular closed-cycle energy storage systems that do not involve the release of CO_2. We present potential energy surfaces for ground states and excited states and discuss the roles that these states play when harvesting, storing, and releasing solar energy. Furthermore, we have illustrated new approaches for obtaining synergy between theoretical modeling and future experimental work.

Introduction

Climate changes demand a shift to clean energy in order to reduce carbon emissions, and solar energy is one of the most promising alternatives to traditional energy sources such as oil, coal, and natural gas. The burning of these fossil fuels can potentially be significantly reduced with a shift to solar heat batteries for low-temperature heating [1]. The dihydroazulene/vinylheptafulvene (DHA/VHF) pair and other photo-/thermo-switches have due to their potential applications as systems for closed-cycle molecular thermal storage of solar energy [2] attracted large interest in recent years [3–9]. The parent DHA/VHF system (2-phenyl-1,8a-dihydroazulene-1,1-dicarbonitrile and its corresponding VHFs, system 1 in Figure 1) is able to store solar energy by the DHA species (1a) absorbing a photon and undergoing electrocyclic ring-opening to an s-cis-VHF (1b). This then undergoes a conformational change to a meta-stable s-trans-VHF (1c) in which energy is stored for a prolonged period of time. This energy can be released by e.g. a temperature increase or Lewis acids [10–12]. The system can thus both absorb solar energy, store it chemically, and release it thermally upon request - hence described as solar heat battteries.

Upon the development of new - and often large - derivatives of the DHA/VHF system, a computationally viable scheme for studying possible alterations to the switching mechanisms is needed. The focus of most computational studies of these switches has been on improving their energy storage capacity or tuning the thermal back-reaction barrier (i.e. the activation energy of the VHF→DHA conversion) [13–21]. Additionally, two detailed studies on the photodynamics of DHA/VHF switches (the parent system [22] and 1,2,3,8a,9-pentahydrocyclopent[a]azulene-9,9-dicarbonitrile (B1a) and its corresponding VHF (B1b) [23], respectively; cf. Figure 1) and two investigations on the main structural components of DHA and VHF, namely azulene [24] and fulvene [25] respectively, have been published over the years.

Quite recently, we have published a paper [26] on a multimode switch (combining the DHA/VHF and DTE/DHB [27–29] switches) in which we used the below procedure to investigate its switching mechanisms. In this work, we review the literature on the DHA/VHF switching mechanism, substantiate the validity of our procedure, and show that density functional theory (DFT) and its time-dependent linear response formalism (TD-DFT) are able to qualitatively reproduce the potential energy surfaces obtained by Boggio-Pasqua and co-workers using CASSCF [23], hence enabling us to extend this procedure and investigate a variety of DHA/VHF systems too large for routine multireference treatment. We present new calculations on the excited states of the systems in Figure 1 including both synthesized (1 [30], B1 [31], 2 [32], 3 [17], and 4[6]) as

Citation: Gertsen AS, Mikkelsen KV. The Switching Mechanisms of Dihydroazulene/Vinylheptafulvene Photo-/Thermoswitches. Japan J Res. 2023;4(6):1-10.

well as model DHA/VHF switches previously published (B2-B4 [23], 6 [17], and 7 [26]) and an unpublished model system (5) and put forward a hypothesis to explain their ring opening/closure mechanisms with references to e.g. orbital symmetry. Using a simple and computationally rather cheap screening method to help qualitatively predict the photoinduced behaviour of DHA/VHF switches, we conclude that the two different types of transition states found by DFT methods in previous work [17,20,21,26] are relevant for different parts of the closed-cycle switching - one for the photoinduced DHA to VHF ring-opening and both for the thermal ring- closure back-reaction depending on the specific system. Furthermore, the TD-DFT results presented herein are in correspondence with experiments on the photodynamics of both the ring-opening and -closure of DHA/VHF systems [10,11,22,31,33,34], why we are confident that this procedure can serve as a cheap alternative to e.g. CASSCF for large systems when only qualitative tendencies are of importance. We do, however, see inconsistencies between our results and the conclusions drawn in ref 34 why we propose a design for a new experiment addressing these. In addition, we propose experiments to verify or falsify our hypotheses of the roles of the two types of transition states we have investigated.

The present work thereby represents important insight in the switching mechanisms of DHA/VHF photo-/thermoswitches and a path for future work on these as well as progress for the DFT design process of new model molecular switches for thermal storage of solar energy, taking us one step closer to efficient solar heat batteries.

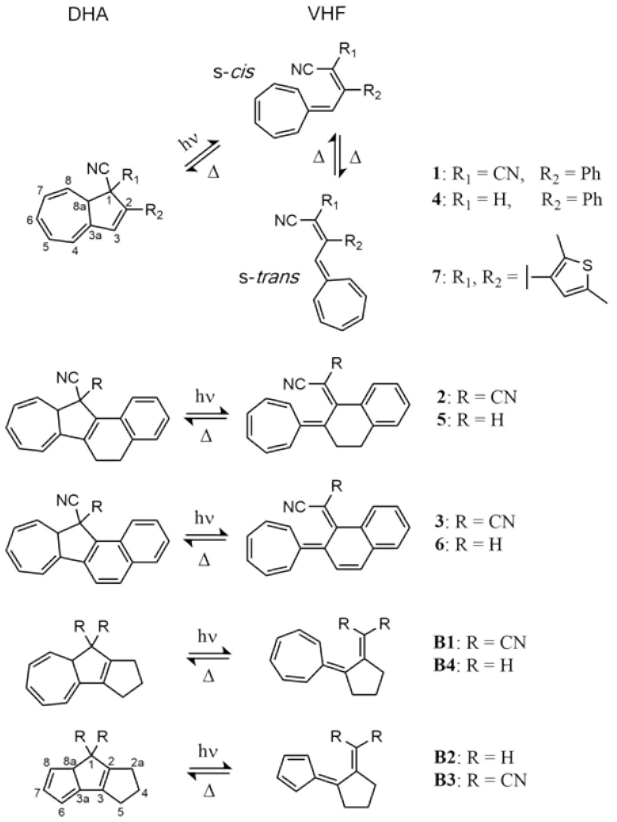

***Figure 1**. Structures of the systems investigated in this work.*

Computational considerations

The potential energy surface plots central to this section are the results of a three-step procedure:

- Location of all relevant transition states (TSs) between the different stereoisomers of the DHAs and VHFs;
- Calculation of intrinsic reaction coordinate paths (IRCs) taking these TSs as starting points and following the ring-opening/-closure reaction coordinate;
- Linear response TD-DFT excitation calculations of each of the non-equilibrium geometries resulting from the IRC calculations.

Going into details, we start off by locating the lowest energy conformer (when single-bond rotations are possible) of the DHA and, if relevant, s-*trans*-VHF by a 3 kcal/mol cut-off rotary search using a genetic algorithm implemented in The Open Babel Package, version 2.4.1 [35]. These are then geometry optimized and confirmed as energy minima by frequency analyses. The transition states of the ring-opening/-closure reactions are located and confirmed as first-order saddle points by frequency analyses too, after which they are used as initial geometries for IRC calculations. These follow the intrinsic reaction coordinate corresponding to the imaginary frequency vibration of the respective TSs, *i.e.* the ring-opening/-closure reaction coordinate, and take a maximum of 100 steps in each direction (in the same and in the opposite direction of the transition vector). We update the force constants every third or fifth step for the TS_T starting geometry and every step for the TS_P starting geometry in general. These IRC paths will thus determine which stereoisomers of the DHAs correspond to which stereoisomers of the VHFs. The hundreds of non-equilibrium geometries calculated along the individual reaction coordinates are then subject to TD-DFT linear response calculations which yield *e.g.* the vertical excitation energies of these. The ground state energy and the first three excited state energies are then plotted as a function of intrinsic reaction coordinate for each of the transitions (see Fig. 4 and SI, Figs. S6-S13). It is important to note that due to the inherent adiabatic approximation in TD-DFT, we obtain the adiabatic potential energy surfaces. Avoided crossing between the ground state PES and the first excited state PES thus leads to the possibility of locating a first order saddle point on the ground state PES in the immediate vicinity of a conical intersection. It is well argued in the literature that the photoinduced ring-opening of some DHA derivatives proceeds through a conical intersection [22,31,36], and hence, we are able to gain some insight in the ring-opening mechanism of DHA/VHF switches without using expensive multireference methods.

In the work of Boggio-Pasqua and co-workers (ref 23), CASSCF is performed on three model systems (**B2-B4**) with a reduced number of π-electrons compared to the system of interest (**B1**) to reduce the computational cost to a feasible level. For the two model systems **B2** (for which they have chosen to present results) and **B3**, the seven-membered ring of **B1** is reduced to a five-membered ring, and additionally for **B2** the cyano groups are interchanged for hydrogens. It is argued in their work with references to refs 24 and 25 that the five- and seven-membered rings are electronically interchangeable, and they do claim to see

the same tendencies for the five- and seven-membered ring systems (**B2** and **B4**, respectively) and for the systems with and without cyano groups (**B3** and **B2**, respectively). They are hence confident that the PESs of **B2** is representative for those of the system of interest, **B1**, but for consistency, we investigate all four compounds herein.

Regarding the DFT methodology, the M06-2X [37] global exchange functional has been shown to model both the ground-state energetics and the UV-vis absorptions of DHA/VHF switches satisfactorily [18], and thus all calculations are performed at the M06-2X/6-311+G(d) level of theory in Gaussian 09 [38]. No solvent models are used, and thermochemical properties are calculated at a temperature of 298.15 K and a pressure of 1 atm. The three main thermochemical properties we discuss are the energy storage capacity, the thermal back-reaction barrier (TBR), and the relative transition state stability. The energy storage capacity is defined as the change in enthalpy, $\Delta H_{\text{storage}} = \Delta H_{\text{VHF}} - \Delta H_{\text{DHA}}$, between the most stable VHF species (s-*trans*-VHF for **1**, **2**, and **5**) and the DHA species, as this corresponds to the thermal energy we are able to release when going from VHF to DHA. In order to compare the energy storage capacity of DHA/VHF systems of different size and substitution pattern, we also list the energy densities, $u = \Delta H_{storage} / M_{DHA}$ *where* M_{DHA} *is the mass of DHA*. The TBRDHA barrier is defined as the activation energy of the VHF→DHA ring-closure reaction and computed as the change in Gibbs free energy, $\Delta G_{\text{TBR}} = \Delta G_{\text{TS}} - \Delta G_{\text{VHF}}$, of the most stable TS and the closest VHF minimum on the IRC curve following the ring- opening/-closure reaction coordinate (s-*cis*-VHF for **1**, **4**, and **7**). It is known that the TBR barriers are slightly overestimated using the M06-2X functional and that results closer to experiment can be obtained using the PBE0[39] hybrid functional [18], but as the TBR barriers are not the main focus of this work, we report results obtained using M06-2X. The relative transition state stability is calculated as the change in Gibbs free energy, $\Delta\Delta G_{\text{TS}} = \Delta G(\text{TS}_\text{P}) - \Delta G(\text{TS}_\text{T})$, of the determined TSs.

Note that systems **B1**-**B4**, **2-3**, and **5-6** are locked systems, *i.e.* an s-*cis*/s-*trans* conformational change is not possible, why only one VHF conformer is relevant for each of these and hence used in the calculation of both energy storage capacity and TBR barrier. Furthermore, since the (8a*R*)- and (8a*S*)-DHAs of systems **1-3** and **B1**-**B4** are enantiomers and hence have the same thermodynamical properties, we restrict ourselves to presenting results only for the (8a*R*) isomers. Similarly, we present thermodynamical data only for the diastereometric pair (1*S*,8a*S*)- and (1*R*,8a*S*)-DHA for systems **4-6**, since the enantiomers of each of the two have the same thermodynamical properties as these.

Results and Discussions

Transition states and stereoisomeric connections

In the interest of maintaining an overview, we will distinguish between the systems which undergo a 10π electrocyclic ring-closure (those with seven-membered rings, henceforward 10π systems, namely **1-7**, **B1**, and **B4**), and the systems that undergo an 8π electrocyclic ring-closure (those with five-membered rings, henceforward 8π systems, namely **B2** and **B3**). All M06-2X/6-311+G(d) optimized geometries are presented in SI, Figs. S17-S89.

In general, we are able to locate two first order saddle points for each of the investigated systems. We introduce a naming of these, TS_P and TS_T, based on the discussion below. The easiest way to distinguish between these two types of TS is by the C1-C8a interatomic distance - it is in general shorter for the TS_T type than for the TS_P type. Furthermore, the infrared intensity for the imaginary frequency eigenmode is significantly larger for the TS_P type than for the TS_T type. Another way to distinguish them is by their geometry. For the TS_P type of the 10π systems, the plane of C1 and its substituents (*e.g.* the two cyano-groups of **1**) is somewhat parallel to that of the seven-membered ring while it for the TS_T is more perpendicular to it. For the 8π systems, the TS_P type now has a plane of C1 and its substituents being perpendicular to the five-membered ring while it for the TS_T type is more parallel to it. As an example, the two types of TSs for the **B1** system are shown in Figure 2, while the geometries for the TSs of the remainder of the systems can be found in SI. We were unable to locate the TS_T type for system **3**, which we expect to be due to the non-flexible geometry and significantly altered electron structure of **3** compared to **1** and **2**. Note that we above have used and henceforth will use the term 'transition state' (TS) for both DFT first order saddle points irregardless of their physical role(s) in the switching mechanism.

Subsequent to locating the TSs, IRC paths of each of them were calculated. To provide an overview over the resulting connections between the different DHA and VHF isomers, we list these for the systems exhibiting diastereomerism in Table 1. The key finding in this table is that the stereoisomeric match between DHAs and VHFs going over TS_P is the exact opposite of the one going over TS_T. Looking into the molecular orbital (MO) symmetry of the (s-*cis*) VHFs, it is seen that the highest occupied MOs (HOMOs) of the 10π systems are out-of-phase around C1 and C8a and in-phase for the 8π systems. The opposite applies to the lowest unoccupied MOs (LUMOs) which are in-phase around C1 and C8a for the 10π system and out-of-phase for the 8π systems (*cf.* Figure 3 and SI, Figs. S1-S5). Hence, in order for the 10π systems to undergo a back-reaction without breaking orbital symmetry, the HOMOs indicate that a thermally activated back-reaction should follow a disrotatory mechanism while the LUMOs indicate that a photochemically activated back-reaction should follow a conrotatory mechanism (with little or no orbital rotation at all as is best seen for the LUMO of (*E*)-**4b** in Fig. 3). The reverse is the case for the 8π systems for which the HOMOs indicate that a thermally activated back-reaction

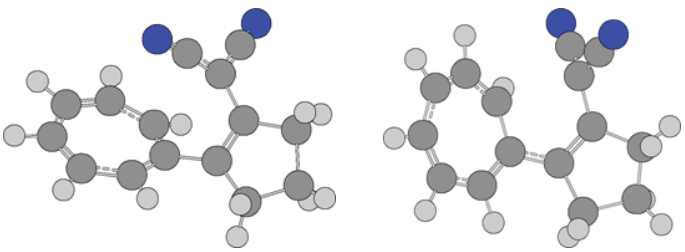

(a) TS_P (b) TS_T

Figure 2. *The two DFT first order saddle points of the B1 system.*

should follow a conrotatory mechanism while the LUMOs indicate that a photochemically activated back-reaction should follow a disrotatory mechanism. Combining this with the knowledge of the two types of transition states and their roles as connection points between specific DHA and VHF stereoisomers (*cf.* Table 1), it is seen that the TS_T type of transition state corresponds to the disrotatory ring-closure of the 10π systems and the conrotatory ring-closure of the 8π systems, why it is given the "T"-subscript to indicate a thermally activated orbital symmetry conserved reaction on the ground state PES. Accordingly, the TS_P type of transition state is seen to correspond to the conrotatory ring-closure of the 10π systems and the synrotatory ring-closure of the 8π systems. A femto-second two-pulse experiment has proven a *para*-cyano substituted derivative of **1b** to be photochemically active [34], hence demonstrating a two-way photochemical reversibility between the DHA and the s-*cis*-VHF. This second type of TS is thus given a "P"-subscript to indicate a photochemically activated orbital symmetry conserved reaction. An indepth discussion of this will be given later in Section 3.3. However, it is well known for the **B1** system that no photochemical back-reaction is seen [31], why we hesitate to conclude anything on the photoactivity of **B1b** but keep the TS_P notation for consistency.

Table 1. *Overview of which diastereomers of the DHA 4a, 5a, or 6a that are connected to which E /Z -configurations of VHF 4b, 5b, or 6b, respectively, through which type of transition state. These connections are confirmed by DFT ground state IRC paths.*

IRCconnection	TSP	TST
(1R,8aR)	(Z)	(E)
(1R,8aS)	(E)	(Z)
(1S,8aR)	(E)	(Z)
(1S,8aS)	(Z)	(E)

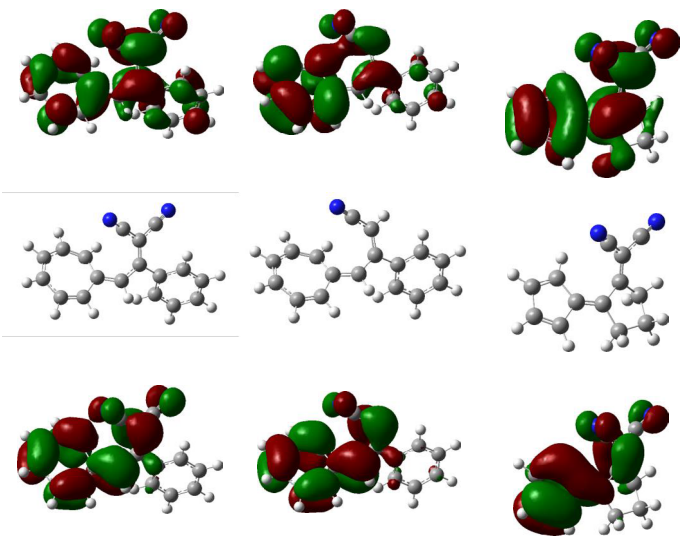

Figure 3. *HOMOs (bottom row) and LUMOs (top row) for 1b, (E)-4b, and B3b (left, middle, and right column, respectively). An isovalue (contour threshold) of 0.02 au is used in the visualization.*

Thermodynamics

Although the TS_P type is dedicated to photoreactions in the above Section 3.1, it is important to remember that this was for reactions with conserved orbital symmetry and that *e.g.* a charge separation could break this orbital symmetry and facilitate a TBR on the ground state PES through this type of TS. Looking at the Mulliken and APT charges (see SI, Table S1), no significant charge separation between C1 and C8a is, however, seen for the TS_P type of the systems with one or no cyano groups on C1 (**4**-**7**, **B2**, and **B4**), while the TS_P type for systems with two cyano groups (**1**-**3**, and **B1**) show a significant C1-C8a charge separation of 1.6-2.1 *e*. This indicates that the substitution pattern on C1 determines the degree of charge separation between this and C8a and that this charge separation is not linked to the type of TS. In spite of this ambiguity with respect to a TBR mechanism *via* charge separation, it is still obvious that the Boltzmann factor is the deciding factor and that it is thus most likely that a TBR will go through the TS with the lowest energy. In Tables 2 and 3, we hence list the relative transition state stabilities and the TBR barriers for each of the investigated systems through their respective lowest TS along with the systems' energy storage capacities and energy densities. A definition of the listed parameters is given in Section 2.

Looking at the energy storage capacities and energy densities, we see, as discussed in ref 17, a remarkable increase in both these parameters relative to the parent system when first locking the s-*cis*/s-*trans* conformational change in system **2** and further by aromatically stabilizing the DHA of system **3**. Removing one cyano group from each of these further increases both the energy storage capacity and energy density as seen for systems **4**, **5**, and **6**, respectively. System **3** remains, to our knowledge, the synthesized DHA/VHF with the highest energy density (neglecting the problems with the photoisomerization of **3a** as discussed in ref 17), and system **6** equally remains, to our knowledge, the model DHA/VHF compound with the highest energy density. Both these systems have, however, quite low TBR barriers (as a reference, **1c** has a half-life of 218 min in MeCN [40] while **2b** has one of 13 ms in EtOH [32]), but for further discussion and improvements on this, we refer to ref 17. More interesting for this work are the tendencies for the relative transition state stability. As seen in Table 2, all di-cyano systems (except for the 8π system **B3** for which the TS_P type is considerably more unstable than TS_T) have a more stable TS_P than TS_T. This, in correspondence with the charge separation analysis above, strongly indicates that the TBR for these di-cyano system will go through the TS_P. Experiments also show a clear dependence of the TBR barrier on solvent polarity for **1**, supporting this conclusion of a charge separated mechanism through TS_P for the TBR [40,41].

For the mono-cyano systems **4**, **5**, and **7**, the TS_T type has significantly lower energy, and these systems will hence undergo a TBR through this type of TS. Interestingly, the TS_P type is considerably more stable than the TS_T type for system **6** why it seems that the number of electron withdrawing groups on C1 not singlehandedly controls the relative TS stability. While locking the s-*cis*/s-*trans* conformational change from **1** to **2** and from **4** to **5** results only in minor changes in relative TS stability and TBR barrier, the reduction of the bridging ethyl from **2** to **3** and from **5** to **6** results in a significant stabilization of the TS_P type of TS and

Table 2. *Relative stability of the two types of transition states TSP and TST, energy storage capacity, and TBR barrier in kJ/mol and energy density in MJ/kg for each of the (8aR)-DHA stereoisomers and their corresponding VHFs of systems 1-3 and B1-B4 and the (1R,8aR)-DHA stereoisomer and its corresponding VHFs of system 7. A positive (negative) ΔΔGTS-value means that TST (TSP) is more stable. aValues from ref 17. bValues from ref 26 (only for the DHA/VHF part of the multimode switch).*

System	1	2	3	B1	B2	B3	B4	7
ΔΔGTS	-5.52	-2.75	n/a	-0.92	132	127	38.6	27.1b
ΔHstorage	35.2	64.7a	114a	22.8	18.5	-0.44	65.3	35.0b
Energy density	0.13	0.23a	0.40a	0.10	0.13	-0.00	0.38	0.09b
ΔGTBR	106	98.1	33.5a	115	121	122	144	116b

Table 3. *Relative stability of the two types of transition states TSP and TST, energy storage capacity, and TBR barrier in kJ/mol and energy density in MJ/kg for each of the (1S,8aS)- and (1R,8aS)-DHA stereoisomers and their corresponding VHFs of systems 4-6. A positive (negative) ΔΔGTS-value means that TST (TSP) is more stable. cValues from ref 17.*

	System	**4**	**5**	**6**
(1S,8aS)	ΔΔGTS	11.0	17.0	-14.3
	ΔHstorage	66.6	84.3	137c
	Energy density	0.29	0.33	0.54c
	ΔGTBR	133	123	81.5
(1R,8aS)	ΔΔGTS	21.3	26.2	-15.0
	ΔHstorage	61.6	86.1	133
	Energy density	0.27	0.33	0.52
	ΔGTBR	123	116	79.7

hence in a major decrease of the TBR barrier. The electronic rearrangement induced by this aromatic stabilization of the DHA-compounds thus seems to be the explanation to this. Having a closer look at the MOs (see SI, Figs. S1 and S2) and comparing them to the data in Tables 2 and 3, the conjugation in the aromatically stabilized systems (**3** and **6**) allows for more of the HOMO electron density to be localized on the phenyl substituent which is in turn believed to be directly connected to the large stabilization of the TS_P type of TS for these systems. Furthermore, the rotation around the C1-C2 double bond of the VHF-compounds needed to reach the ground state TS_T geometry with in-phase C1-C8a MOs has a barrier that is possible to modify moderately, but the possibility of strongly tuning the stability of the TS_P by relatively small modifications may widen the spectra of possible controlled heat release schemes.

To summarize, it is hypothesized that larger conjugation of DHA/VHF systems stabilizes the TS_P and hence lowers the TBR barrier (if this is to be more stable than the TS_T type of course). This is in correspondence with experiments that show a greatly reduced half-life of a 3-phenyl substituted version of **1**; while system **1** has a half-life of 218 min in MeCN as mentioned above, the 3-phenyl substituted version has one of 14 s in MeCN [42]. Furthermore, the relative energies of the two types of transition states, TS_P and TS_T, can be controlled with minor structural modifications not affecting the general characteristics of these, enabling an easy design of experiments aiming to confirm the predictions made in this section. An experimental investigation of the hypothesis of C1-C8a charge separation being independent of TS type but mainly dependent on C1 substitution pattern would for example be interesting. By substituting a variety of electron withdrawing and electron donating groups onto C1, the relation between solvent polarity and TBR barrier could indicate if a charge separated mechanism is followed [40,41], while it in concert with quantum chemical calculations determining the TS type from the MOs could verify or falsify this.

Excited state dynamics

Following the procedure presented in Section 2, we have investigated the DFT potential energy surfaces of the DHA/VHF systems **B1**-**B4** and **1**-**7**. These are visualized in Figure 4 (for systems **1** (top panel), **4** (middle panel), and **B1** (bottom panel)) and in SI, Figs. S6-S13 (for the remainder of the systems). If we start off by summarizing the experimental literature on the DHA/VHF switching mechanisms, it is known for the parent system **1** and its derivatives that a shallow minimum is present on the first singlet excited PES of DHA (^{1}DHA*) and that there is an activation barrier between this ^{1}DHA* PES and that of the s-*cis*-VHF [10,33]. This is given by the fact that one can observe a DHA fluorescence whose quantum yield increases with decreasing temperature while the ring-opening quantum yield decreases with decreasing temperature [10,33]. Furthermore, both a triplet and a biradicaloid ring-opening mechanism can be excluded, confirming that the DHA undergoes a ring-opening through an electron delocalized ^{1}DHA* intermediate [10,11]. The ring-opening itself, *i.e.* ^{1}DHA*→^{1}s-*cis*-VHF*, is then followed by an internal conversion to the s-*cis*-VHF (**1b**) [33,36] which, as mentioned earlier, undergoes a conformational change to the s-*trans*-VHF (**1c**). Regarding the back-reaction, it

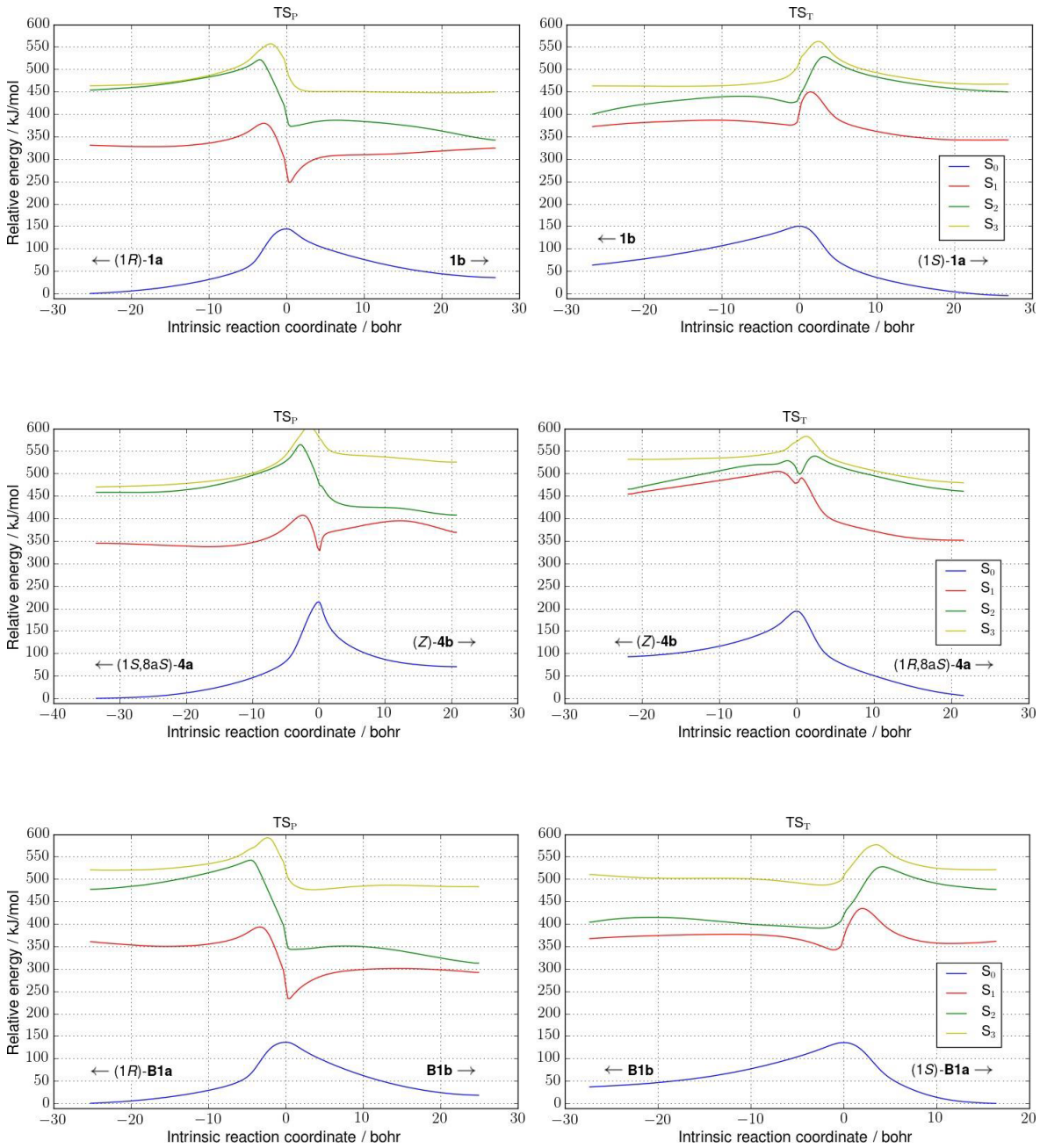

Table 4. *Comparison between the potential energy, UFC→M, of the Franck-Condon DHA state (FC- 1DHA*) relative to the 1DHA* minimum (M-1DHA*) and the S1 activation barrier, Ea*, of the 1DHA*→1s-cis-VHF* (or 1VHF*) ring-opening estimated from the TD-DFT PES plots (Fig. 4 and SI, Figs. S6-S13). All values are TD-DFT electronic energies in eV.*

is well known to proceed thermally [10,30], but as discussed above, it has been proven that it can be photoinduced from the s-*cis*-VHF too [34,36]. The lack of photoactivity from the s-*trans*-VHF is often dedicated to a "free-rotor" effect in the literature [43,44], and conical intersections accounting for this type of internal conversion have been located in theoretical studies using CASSCF on both system **1** [22] and **B1** [23].

Regarding the **B1** switch, the same characteristics (^{1}DHA* minimum and a barrier between this and the VHF) are present for the ring-opening reaction [31] but an important difference between this and **1** is the one in ring-opening quantum yield. For **B1**, it is close to unity [31] while it for **1** is 0.35-0.60 depending on solvent [10]. Both experiments [10] and theory [23] indicate that this discrepancy can be explained by the ring-opening of **B1** proceeding all the way from ^{1}DHA* through a conical intersection to the VHF S_0 and by the ring-opening of **1** having both a short- and a long-lived component dedicated to the ring-opening ^{1}DHA*⟶^{1}s-*cis*-VHF* itself and to an internal conversion from ^{1}s-*cis*-VHF* to the s-*cis*-VHF S_0, respectively [33,36]. These findings are elegantly presented in ref 36 where ultrafast time resolved spectroscopy in concert with two-pulse/two-color measurements is used to investigate the switching mechanisms of both **1** and **B1**.

Moving to the TD-DFT PES plots in Fig. 4, it is seen in the left panels that a 1DHA* minimum and a barrier on the S_1 PES is present for all systems. This is followed by a sharp minimum

on the S_1 PES at the same IRC value as the TS_P, resulting in the S_1 and S_0 states lying close in energy, making a fast internal conversion highly probable. As discussed in Section 2, the lack of a multireference description in DFT prevents us from seeing actual state crossings, but we are certainly able to see indications of these. Comparing the left panels to the right, it is seen that the S_1 PESs in the vicinity of the TS_T type generally have higher activation barriers and no pronounced sharp minima at the same IRC values as TS_T. These observations clearly indicate that the ring-opening of the DHA/VHF systems happens on the reaction coordinate of the TS_P type first order saddle point and that no photoisomerization is expected from the excited states in the vicinity of TS_T.

Regarding the photochemically induced back-reaction of a *para*-cyano substituted version of **1b** proven in ref 34, we see for system **1** (top panel of Figure 4) that an energetic pathway from FC-^{1}**1b*** towards the S_1 minimum is present in this reaction coordinate, indicating that the TS_P reaction coordinate accounts for this behavior too. Similar tendencies are observed for systems **2-3** and **5-7**, while **4** and the **B1-B4** range of systems seem to have a ^{1}VHF* PES sloping away from the S_1 minimum in the TS_P reaction coordinate plots (left panels). To investigate this, we have geometry optimized the ^{1}s-*cis*-(*Z*)-VHF* of system **4** and the ^{1}VHFs* of systems **B1-B4**. As expected, no minima were found. For comparison, the geometry optimizations of ^{1}s-*cis*-VHF* and ^{1}s-*trans*-VHF* of system **1** did not converge to minima either. This is in correspondence with experiments detecting no fluorescence of the VHFs of either of the systems **1** or **B1** [10,23,31]. However, we be came aware that these optimizations of the S_1 VHF geometries actually accounted for the"freerotor" effect mentioned above. Upon relaxation from the FC-state, the electron distribution shifts such that the exocyclic C3-C3a double-bond of the ground state VHF is broken, thus making the seven membered ring free to rotate and through this rotational motion transfer the energy from the excitation to the environment. As seen in SI, Figs. S14-S16, plotting the dihedral angle of this rotation, D(C2,C3,C3a,C4), versus the TD-DFT excitation energy for VHFs **1b**, **1c**, and **B1b** indicates that the two parameters are in strong correspondence and that rotation around this exocyclic C3-C3a bond upon excitation most likely is responsible for the lack of photoactivity of the VHFs. This effect is furthermore indicated by the molecular orbitals of the systems (*cf.* Fig. 3 and SI, Figs. S1-S5) where it is seen that a nodal plane is introduced at the C3-C3a bond in the LUMOs, making the rotation of the large seven (or five) membered rings possible. Furthermore, we see indications of a C2-C3 double bond forming in the VHF S_1 states (also obvious from the LUMOs), which makes the barrier for the s-*cis*/s-*trans* conformational change for system **1** and **4** significantly larger on the S_1 surface than on the S_0 (ground state) surface. A photochemically mediated s-*cis*/s-*trans* conformational change is hence not possible. This is in correspondence with the CASSCF results and discussions in ref 22.

It is interesting that this "free-rotor" effect described above is seen for both the s-*cis*-VHF and s-*trans*-VHF of system **1**, as the s-*cis*-VHF is from experiments expected to be photoactive [34]. The two-pulse experiments described in refs 34 and 36 are carried out by hitting the DHA with a 340 nm pulse and subsequently with a 530 nm pulse delayed by 25 ps from the first. The first pulse triggers the DHA→s-*cis*-VHF ring-opening, while the second pulse excites the s-*cis*-VHF and induces a photochemically activated ring-closure (the s-*cis*-VHF→DHA back- reaction). Since our results suggest that the "free-rotor" effect is relevant when exciting the minimum s-*cis*-VHF structure, it would be most interesting to have these time-resolved two-pulse experiments carried out with a series of different pulse delays to investigate if the photoinduced ring-closure is dependent on this delay. It is obvious that if the sum of the FC-^{1}DHA*→M-^{1}DHA* relaxation time (100 fs [34]), the M-^{1}DHA*→^{1}s-*cis*-VHF* ring-opening time (1.2 ps[33]), the ^{1}s-*cis*- VHF*→s-*cis*-VHF internal conversion time (15 ps [33,34]), and the relaxation time of this non-relaxed s-*cis*-VHF to its minimum is larger than the pulse delay of 25 ps, it is not the minimum s-*cis*-VHF structure that one has proven to be photoactive, but a non-relaxed s-*cis*-VHF. From the time-scales listed, this seems to be a plausible situation. Thus, a series of different pulse delays could determine whether the vertically excited minimum s-*cis*-VHF (FC-^{1}s-*cis*-VHF*) state lies on a reaction coordinate before or after a local maximum on the S_1 surface and hence whether or not it slopes towards or away from the TS_P reaction coordinate and in turn if the minimum s-*cis*-VHF is photoactive or not, respectively. We expect, based on our calculations, that this minimum s-*cis*-VHF is not photoactive. The time of the s-*cis*-VHF→s-*trans*-VHF conformational change has experimentally been determined to be 10 μs [36], leaving the system in the s-*cis*-VHF state long enough to carry out the proposed experiments. If we are wrong and the minimum s-*cis*-VHF is indeed photoactive, it would presumably demand a much faster s-*cis*-VHF→s-*trans*-VHF conformational change to prevent photochemically induced back-reactions that would otherwise lower the overall ring-opening quantum yield significantly. We strongly urge that these experiments are carried out.

One characteristic that the PES plots in Figure 4 do not capture is the need of the Frank-Condon DHA state (FC-^{1}DHA*) to have a potential energy sufficient to overcome the S_1 activation barrier. Simply put, the difference between the FC-^{1}DHA* and the ^{1}DHA* minimum (M-^{1}DHA*) should be larger than the S_1 activation barrier, E_a* in order for this FC state to be able to gain enough kinetic energy upon nuclear relaxation to climb this. The reason that this effect is not captured is that only one reaction coordinate, the ring-opening/-closure reaction coordinate, is plotted. However, TD-DFT with the M06-2X functional can nicely capture this effect by an S_1 geometry optimization of the ^{1}DHA* (and subsequent excited state frequency analysis to confirm its nature as a minimum), which is then related to the vertical excitation energy and compared to E_a* estimated from the plots in Fig. 4. As seen in Table 4, all systems have sufficient energy to overcome this barrier and thus undergo ring-opening. This is consistent with the tendencies found for the **B1**-**B4** range of systems with dynamics calculations in ref 23.

Interestingly, we furthermore see a relation between the calculated S_1 activation barriers, E_a*, for the ring-openings of the systems and their measured ring- opening quantum yields, $\Phi_{DHA\rightarrow VHF}$. While the values for **B1** is $\Phi_{\mathbf{B1a\rightarrow B1b}} \sim 1$ and $E_a^*{}_{\mathbf{B1}}$ = 0.45 eV, the ones for **1** is $\Phi_{\mathbf{1a\rightarrow 1b}}$ = 0.55 (in MeCN) and $E_a^*{}_{\mathbf{1}}$ = 0.54 eV. It is hence expected that *e.g.* the model system **5** would have a quantum yield lower than these (*cf.* Table 4). We would of course need more data-points to substantiate this hypothesis of the ring-opening quantum yield being related to the S_1 activation barrier and furthermore include solvent effects in our calculations, but to our knowledge, ring-opening quantum yields of the remainder of the synthesized systems have not been published, while solvent effects are not in the scope of this work. It would, however be an interesting subject for future

investigations.

To summarize, all experimental findings regarding the switching mechanisms of the parent system **1** can be reproduced qualitatively with plots as those in Fig. 4 using TD-DFT: Both the ^{1}DHA* minimum, the S_1 activation barrier for the ring-opening, the closely lying S_1 and S_0 PESs enabling fast internal conversion, the possibility of a photoinduced back-reaction, and the transition state for the thermally activated orbital symmetry conserved back-reaction, TS_T, are found.

Additionally, the second type of DFT first order saddle point located, namely TS_P, is not only found to be relevant for the DHA to VHF photoisomerization, but also for a back-reaction mediated by a charge separation which is fully consistent with the known behavior of this system (**1**) [40,41]. In addition, there are indications that this procedure enables comparison of *e.g.* ring-opening quantum yields across systems. We have thus shown that DFT with the global exchange functional M06-2X performs quite well for characteristics that normally would require multireference methods for a full description. In order to visually sum up the complete switching mechanism of DHA/VHF switches, we have condensed both the new findings pre- sented in this work as well as the results from experiments and previous theoretical studies in a single graphic (Figure 5).

Reading the figure from the left (the TS_P IRC axis), we excite the ground state DHA species to its Franck-Condon state (FC-^{1}DHA*). Upon relaxation to the excited state DHA-like minimum (M-^{1}DHA*), it has gained enough kinetic energy to overcome the ring-opening activation barrier on the S_1 surface and cross to a ^{1}s-*cis*-VHF* state. This then undergoes a fast internal conversion to the ground state s-*cis*-VHF due to the closely lying S_1 and S_0 potential energy surfaces near the TS_P reaction coordinate. Four scenarios are possible from this ground state s-*cis*-VHF: **i)** A photochemically activated and orbital symmetry conserved back-reaction to the DHA when exciting the s-*cis*-VHF prior to full relaxation (orange arrows); **ii)** excitation of the minimum s-*cis*-VHF structure resulting in an internal conversion back to its ground state by transferring energy to the environment *via* the "free-rotor" effect (green arrows); **iii)** a thermally activated conformational change to the s-*trans*-VHF; and **iv)** a thermally activated back-reaction through TS_P (possibly by a charge separated mechanism resulting in an orbital symmetry broken transition structure). The s-*trans*-VHF is not photoactive and recrosses to its ground state through the "free-rotor" effect. Hopping to the right axis (IRC of TS_T), we note that the two s-*trans*-VHF states, although plotted on separate axes, are fully equivalent. This s-*trans*-VHF can undergo a thermally activated conformational change to the s-*cis*-VHF, which then can undergo a thermally activated and orbital symmetry conserved back-reaction to DHA through TS_T on the ground state. It is important to note that the S_1 state at the TS_T IRC axis is higher in energy than it is at the TS_P IRC axis, why it slopes towards this. Exciting the DHA near the TS_T reaction coordinate will thus result in an out-of-plane relaxation of the FC-^{1}DHA* in the direction of the ^{1}DHA* minimum near the TS_P reaction coordinate, and the switching cycle can thus repeat itself.

Concluding remarks

We have in this work investigated a variety of DHA/VHF photo-/thermoswitches with the intend to determine a viable method for screening the switching mechanisms of these and related systems. Using density functional theory, we have been able to reproduce the vast majority of experimental findings and tendencies from multireference calculations, demonstrating the wide applicability of the M06-2X functional. By reviewing two decades of literature on DHA/VHF systems and contributing with new calculations, a full overview of the DHA/VHF switching mechanisms is given and summarized in a single

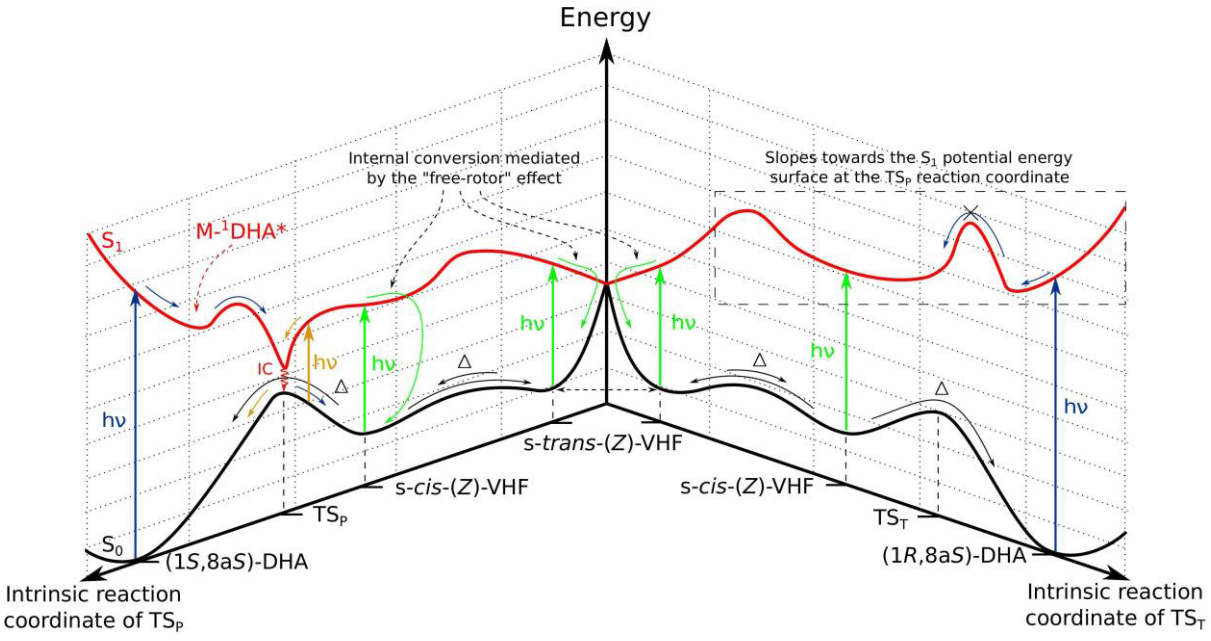

***Figure 5**. Qualitative three-dimensional schematic of the full switching mechanisms of DHA/VHF photo-/thermoswitches.*

figure (Figure 5). This work hence represents an important step forward in the design process of new photo-/thermoswitches for use in closed-cycle molecular solar thermal storage systems (solar heat batteries) as the computational method devised here serves as a cheap alternative to multireference calculations.

This work should furthermore motivate new and further experiments on both the photodynamics and thermally activated back-reactions of DHA/VHF systems. First of all, we have questioned whether or not the minimum s-cis-VHF is photoactive as concluded in ref 34 from sub-30 fs two-pulse experiments. We propose new experiments with a series of different pulse delay times to address this discussion. Second of all, the nature of the TSP DFT first order saddle point, which is hypothesized to have relevance for both the ring-opening and -closure mechanisms for certain systems, should be investigated experimentally. A design for such an experiment is proposed too. We urge that these are carried out in order to find the last few pieces of the puzzle that is the switching mechanism of one of the most promising type of system for solar heat batteries.

Acknowledgments

The authors thank the Center for Exploitation of Solar Energy at University of Copenhagen and Danish e-Infrastructure Cooperation for financial support and MSc. Benjamin N. Frandsen, MSc. Anders B. Skov, and Prof. Dr. Mogens Brøndsted Nielsen for fruitful discussions.

Supporting information

Table of C1-C8a charge separation; molecular orbitals (HOMO and LUMO) for all VHFs; DFT potential energy surface plots for all remaining systems; plots accounting for the ”freerotor” effect; optimized geometries for all systems

References

1. Kucharski TJ, Tian Y, Akbulatov S, Boulatov R. Chemical solutions for the closed-cycle storage of solar energy. Energy Environ Sci. 2011;4;4449–4472.
2. Yoshida ZI. New molecular energy storage systems. J Photochem. 1985;29(1):27–40.
3. Feng Y, Liu H, Luo W, et al. Covalent functionalization of graphene by azobenzene with molecular hydrogen bonds for longterm solar thermal storage. Sci Rep. 2016;3:3260.
4. Kucharski TJ, Ferralis N, Kolpak AM, Zheng JO, Nocera DG, Grossman JC. Templated assembly of photoswitches significantly increases the energy-storage capacity of solar thermal fuels. Nat Chem. 2014;6(5):441-447.
5. Broman SL, Nielsen MB. Dihydroazulene: From controlling photochromism to molecular electronics devices. Phys Chem Chem Phys. 2014;16:21172–21182.
6. Cacciarini M, Skov AB, Jevric M, et al. Towards solar energy storage in the photochromic dihydroazulene-vinylheptafulvene system. Chemistry. 2015;21(20):7454-7461.
7. Fihey A, Perrier A, Browne WR, Jacquemin D. Multiphotochromic molecular systems. Chem Soc Rev. 2015;44:3719–3759.
8. Lennartson A, Roffey A, Moth-Poulsen K. Designing photoswitches for molecular solar thermal energy storage. Tetrahedron Lett. 2015;56(12):1457–1465.
9. Quant M, Lennartson A, Dreos A, et al. Low Molecular Weight Norbornadiene Derivatives for Molecular Solar-Thermal Energy Storage. Chemistry. 2016;22(37):13265-13274.
10. Görner H, Fischer C, Gierisch S, Daub J. Dihydroazu- lene/vinaylheptafulvene photochromism - effects of substituents, solvent, and temperature in the photorearrangement of dihydroazulenes to vinylheptaful- venes. J Phys Chem. 1993;97:4110–4117.
11. Görner H, Fischer C, Daub J. Photoreaction of dihydroazulenes into vinylheptafulvenes: photochromism of nitrophenyl-substituted derivatives. J Photoch Photobio A. 1995;85(3):217–224.
12. Parker CR, Tortzen CG, Broman SL, Schau-Magnussen M, Kilså K, Nielsen MB. Lewis acid enhanced switching of the 1,1-dicyanodihydroazulene/vinylheptafulvene photo/thermoswitch. Chem Commun (Camb). 2011;47(21):6102-6104.
13. Broman SL, Petersen MA, Tortzen CG, Kadziola A, Kilså K, Nielsen MB. Arylethynyl derivatives of the dihydroazulene/vinylheptafulvene photo/thermoswitch: tuning the switching event. J Am Chem Soc. 2010;132(26):9165-9174.
14. Vlasceanu A, Broman SL, Hansen AS, et al. Solar thermal energy storage in a photochromic macrocycle. Chem Eur J. 2016;22(31):10796–10800.
15. Cacciarini M, Jevric M, Elm J, Petersen AU, Mikkelsen KV, Nielsen MB. Fine-tuning the lifetimes and energy storage capacities of meta-stable vinylheptafulvenes via substitution at the vinyl position. RSC Adv. 2016;6: 49003–49010.
16. Petersen AU, Broman SL, Olsen ST, et al. Controlling two-step multimode switching of dihydroazulene photoswitches. Chem Eur J. 2015;21(10):3968–3977.
17. Skov AB, Broman SL, Gertsen AS, et al. Aromaticity-controlled energy storage capacity of the dihydroazulene-vinylheptafulvene photochromic system. Chem Eur J. 2016;22(41):14567–14575.
18. Olsen ST, Elm J, Storm FE, et al. Computational methodology study of the optical and thermochemical properties of a molecular photoswitch. J Phys Chem A. 2015;119(5):896-904.
19. Shahzad N, Nisa RU, Ayub K. Substituents effect on thermal electrocyclic reaction of dihydroazulene–vinylheptafulvene photoswitch: A DFT study to improve the photoswitch. Struct Chem. 2013;24(6):2115–2126.
20. Hansen MH, Elm J, Olsen ST, et al. Theoretical Investigation of Substituent Effects on the Dihydroazulene/Vinylheptafulvene Photoswitch: Increasing the Energy Storage Capacity. J Phys Chem A. 2016;120(49):9782-9793.
21. Ree N, Hansen MH, Gertsen AS, Mikkelsen KV. Density Functional Theory Study of the Solvent Effects on Systematically Substituted Dihydroazulene/Vinylheptafulvene Systems: Improving the Capability of Molecular Energy Storage. J Phys Chem A. 2017;121(46):8856-8865.
22. Schalk O, Broman SL, Petersen MÅ, et al. On the condensed phase ring-closure of vinylheptafulvalene and ring-opening of gaseous dihydroazulene. J Phys Chem A. 2013;117(16):3340-3347.
23. Boggio-Pasqua M, Bearpark MJ, Hunt PA, Robb MA. Dihydroazulene/vinylheptafulvene photochromism: a model for one-way photochemistry via a conical intersection. J Am Chem Soc. 2002;124(7):1456-1470.
24. Bearpark MJ, Bernardi F, Clifford S, et al. The azulene S1 state decays via a conical intersection: A CASSCF study with MMVB dynamics. J Am Chem Soc. 1996;118(1):169–175.
25. Bearpark MJ, Bernardi F, Olivucci M, Robb MA, Smith BR. Can fulvene S1 decay be controlled? A CASSCF study with MMVB dynamics. J Am Chem Soc. 1996;118(22):5254–5260.
26. Gertsen AS, Olsen ST, Broman SL, Nielsen MB, Mikkelsen KV. A DFT study of multimode switching in a combined DHA/VHF-DTE/DHB system for use in solar heat batteries. J Phys Chem C. 2017;121(1): 195–201..
27. Gilat SL, Kawai SH, Lehn JM. Light-triggered electrical and optical switching devices. J Chem Soc Chem Commun. 1993;1993:1439–1442.
28. Irie M, Mohri M. Thermally irreversible photochromic systems. Re- versible photocyclization of diarylethene derivatives. J Org Chem. 1988;53(4):803–808.
29. Irie M. Diarylethenes for memories and switches. Chem Rev. 2000;100(5):1685–1716.
30. Daub J, Knöchel T, Mannschreck A. Photosensitive dihydroazulenes with chromogenic properties. Angew Chem Int Edit. 1984;23(12): 960–961.
31. Ern J, Petermann M, Mrozek T, Daub J, Kuldova K, Kryschi C. “Dihydroazulene/vinylheptafulvene photochromism: Dynamics of the photo- chemical ring-opening reaction. Chem Phys. 2000;

259(2–3):331–337.
32. Broman, SL, Kushnir, O, Rosenberg, M, Kadziola, A, Daub, J & Nielsen, MB. Dihydroazulene/vinylheptafulvene photoswitch: Ultrafast back re- action induced by dihydronaphthalene annulation. Eur J Org Chem. 2015;2015(19):4119–4130.
33. De Waele V, Beutter M, Schmidhammer U, Riedle E, Daub J. Switching dynamics of the photochromic 1,1-dicyano-2-(4-cyanophenyl)-1,8a- dihydroazulene probed by sub-30 fs spectroscopy. Chem Phys Letters. 2004;390(4–6):328–334.
34. De Waele V, Schmidhammer U, Mrozek T, Daub J, Riedle E. Ultrafast bidirectional dihydroazulene/vinylheptafulvene (DHA/VHF) molecular switches: photochemical ring closure of vinylheptafulvene proven by a two-pulse experiment. J Am Chem Soc. 2002;124(11):2438-2439.
35. O'Boyle NM, Banck M, James CA, Morley C, Vandermeersch T, Hutchison GR. Open Babel: An open chemical toolbox. J Cheminf. 2011;3(1):33.
36. Schmidhammer U, Waele VD, Buntinx G, Riedle E. Dihydroazulene molecular switches: Via ultrafast spectroscopy to the first bidirectional switch. In Femtochemistry and Femtobiology (M. M. Martin and J. T. Hynes, eds.), Amsterdam: Elsevier, 2004; pp. 279 – 282.
37. Zhao Y, Truhlar DG. The M06 suite of density functionals for main group thermochemistry, thermochemical kinetics, noncovalent interactions, ex- cited states, and transition elements: Two new functionals and systematic testing of four M06-class functionals and 12 other functionals. Theor Chem Acc. 2008;120:215–241.
38. Frisch MJ, Trucks GW, Schlegel HB, et al. Gaussian 09 Revision E.01. Gaussian Inc. Wallingford CT 2009.
39. Adamo C, Barone V. Toward reliable density functional methods without adjustable parameters: The PBE0 model. J Chem Phys. 1999; 110:6158–6169.
40. Broman SL, Brand SL, Parker CR, et al. Optimized synthesis and detailed NMR spectroscopic characterization of the 1,8a-dihydroazulene-1,1- dicarbonitrile photoswitch. ARKIVOC. 2011; 9:51–67.
41. Spreitzer H, Daub J. Functional dyes for molecular switching. Dihy- droazulene/vinylheptafulvene photochromism: Effect of pi-arylenes on the switching behavior. Liebigs Ann. 1995;9:1637–1641.
42. Mrozek T, Gorner H, Daub J. Multimode-photochromism based on strongly coupled dihydroazulene and diarylethene. Chem Eur J. 2001;7(5):1028–1040.
43. Zimmerman HE, Kamm KS, Werthemann DP. Mechanisms of electron demotion. Direct measurement of internal conversion and intersys- tem crossing rates. Mechanistic organic photochemistry. J Am Chem Soc. 1975;97(13):3718–3725.
44. Sugihara Y, Wakabayashi S, Murata I, et al. Upper excited state reactivity and fluorescence of fused 8- cyanoheptafulvenes. J Am Chem Soc. 1985;107(21): 5894–5897.